

# Metabolic Oscillations in Pancreatic Islets Depend on the Intracellular $\text{Ca}^{2+}$ Level but Not $\text{Ca}^{2+}$ Oscillations

Matthew J. Merrins,<sup>†</sup> Bernard Fendler,<sup>‡</sup> Min Zhang,<sup>¶</sup> Arthur Sherman,<sup>||</sup> Richard Bertram,<sup>§</sup> and Leslie S. Satin<sup>†\*</sup>

<sup>†</sup>Department of Pharmacology and Brehm Diabetes Center, University of Michigan Medical School, Ann Arbor, Michigan; <sup>‡</sup>Department of Physics and <sup>§</sup>Department of Mathematics and Programs in Neuroscience and Molecular Biophysics, Florida State University, Tallahassee, Florida; <sup>¶</sup>Department of Pharmacology, Virginia Commonwealth University, Richmond, Virginia; and <sup>||</sup>Laboratory of Biological Modeling, National Institute of Diabetes and Digestive and Kidney Diseases, National Institutes of Health, Bethesda, Maryland

**ABSTRACT** Plasma insulin is pulsatile and reflects oscillatory insulin secretion from pancreatic islets. Although both islet  $\text{Ca}^{2+}$  and metabolism oscillate, there is disagreement over their interrelationship, and whether they can be dissociated. In some models of islet oscillations,  $\text{Ca}^{2+}$  must oscillate for metabolic oscillations to occur, whereas in others metabolic oscillations can occur without  $\text{Ca}^{2+}$  oscillations. We used NAD(P)H fluorescence to assay oscillatory metabolism in mouse islets stimulated by 11.1 mM glucose. After abolishing  $\text{Ca}^{2+}$  oscillations with 200  $\mu\text{M}$  diazoxide, we observed that oscillations in NAD(P)H persisted in 34% of islets ( $n = 101$ ). In the remainder of the islets (66%) both  $\text{Ca}^{2+}$  and NAD(P)H oscillations were eliminated by diazoxide. However, in most of these islets NAD(P)H oscillations could be restored and amplified by raising extracellular KCl, which elevated the intracellular  $\text{Ca}^{2+}$  level but did not restore  $\text{Ca}^{2+}$  oscillations. Comparatively, we examined islets from ATP-sensitive  $\text{K}^+$  ( $\text{K}_{\text{ATP}}$ ) channel-deficient  $\text{SUR1}^{-/-}$  mice. Again NAD(P)H oscillations were evident even though  $\text{Ca}^{2+}$  and membrane potential oscillations were abolished. These observations are predicted by the dual oscillator model, in which intrinsic metabolic oscillations and  $\text{Ca}^{2+}$  feedback both contribute to the oscillatory islet behavior, but argue against other models that depend on  $\text{Ca}^{2+}$  oscillations for metabolic oscillations to occur.

## INTRODUCTION

Plasma insulin levels are normally pulsatile in mice, rats, dogs, and humans (1–5), and oscillatory periods of 4–5 min are observed when blood is sampled from the hepatic portal vein (4,5). These oscillations are due to the oscillatory activity of individual pancreatic islets (2,6), and insulin pulsatility is disturbed or lost in type 2 diabetics and their near relatives (7–9).

The origin of oscillatory islet activity has been debated since the first reports of periodic islet electrical activity (10). The discovery of ATP-sensitive  $\text{K}^+$  channels ( $\text{K}_{\text{ATP}}$  channels) in  $\beta$ -cells (11,12) raised the possibility that glucose metabolism may be oscillatory and act through  $\text{K}_{\text{ATP}}$  channels to induce oscillations in  $\beta$ -cell electrical activity (13). This idea was given credence by later findings that factors associated with glucose metabolism are often oscillatory, and exhibit periods in the range observed for electrical bursting and oscillations in the cytosolic  $\text{Ca}^{2+}$  concentration or insulin. In particular, oscillations have been observed in oxygen consumption (14–17), NAD(P)H (18), mitochondrial membrane potential (19,20), ATP or the ATP/ADP ratio (21–23) and lactate release (24).

Although it is generally accepted that both cytosolic  $\text{Ca}^{2+}$  and metabolism oscillate in islets, there is disagreement over which is primary and how they interact. Two general classes of models have emerged. In one,  $\text{Ca}^{2+}$  oscillations are essential for metabolic oscillations to occur; in the other, meta-

bolic oscillations can persist in the absence of  $\text{Ca}^{2+}$  oscillations. Models of the first class, whether qualitative or mathematical, are based on the reduction of mitochondrial membrane potential by the flux of  $\text{Ca}^{2+}$  across the mitochondrial inner membrane (25,26), the stimulation of mitochondrial dehydrogenases by  $\text{Ca}^{2+}$  (27,28), or the reduction of cytosolic ATP levels by ATP used for the pumping of  $\text{Ca}^{2+}$  by  $\text{Ca}^{2+}$ -ATPases (29–31). In the models of Fridlyand et al. (32,33),  $\text{Ca}^{2+}$  oscillations can occur in the absence of metabolic oscillations, but metabolic oscillations only occur in the presence of  $\text{Ca}^{2+}$  oscillations. Models of the second class are based on the hypothesis that oscillations are inherent to glycolysis (34–37) or some point downstream of glycolysis, such as mitochondria (28). We refer to these as intrinsic metabolic oscillations.

A key question is whether metabolic oscillations, which occur in the presence of stimulatory glucose and are normally accompanied by  $\text{Ca}^{2+}$  oscillations, can persist in the absence of  $\text{Ca}^{2+}$  oscillations? Previous measurements of islet oxygen consumption ( $\text{pO}_2$ ) revealed large  $\text{pO}_2$  oscillations that were terminated by the  $\text{K}_{\text{ATP}}$  channel-opener diazoxide (Dz) (15). Dz hyperpolarizes the islet and thus terminates islet  $\text{Ca}^{2+}$  oscillations by abolishing  $\text{Ca}^{2+}$  channel activation. The same result was obtained when islet NAD(P)H fluorescence was used as an assay for metabolic oscillations (18). The conclusion drawn from these experiments was that  $\text{Ca}^{2+}$  oscillations drive metabolic oscillations, because the latter oscillations stopped when the former were inhibited. However, there is evidence that oscillations in  $\text{K}_{\text{ATP}}$ ,  $\text{pO}_2$ , or insulin persist in basal glucose (38), or in low  $\text{Ca}^{2+}$  (16,17).

Submitted February 2, 2010, and accepted for publication April 6, 2010.

\*Correspondence: lsatin@umich.edu

Editor: Randall L. Rasmusson.

© 2010 by the Biophysical Society  
0006-3495/10/07/0076/9 \$2.00

doi: 10.1016/j.bpj.2010.04.012

We report that although Dz can eliminate islet metabolic oscillations, monitored as NAD(P)H fluorescence, in many islets the metabolic oscillations persisted. Our model of islet oscillatory behavior, the dual oscillator model (DOM), predicts that in islets where Dz blocked oscillations in NAD(P)H, subsequently raising intracellular  $\text{Ca}^{2+}$  could restore the oscillations in metabolism without restoring  $\text{Ca}^{2+}$  oscillations. We confirm this in the majority of cases tested in this study. Oscillations in NAD(P)H were also clearly evident in sulfonylurea receptor 1 (SUR1) null mice lacking functional  $\text{K}_{\text{ATP}}$  channels, which under the conditions we chose lack oscillations in  $\text{Ca}^{2+}$  or rhythmic electrical activity. These data establish that  $\text{Ca}^{2+}$  oscillations are not essential for metabolic oscillations to occur, and provide support for models in which islet metabolic oscillations are intrinsic, either at the level of glycolysis or at a later step in the metabolic pathway. Unlike earlier studies, we believe these results: 1), unify previous, and seemingly discrepant experimental observations in the islet literature; and 2), are predicted by a single model (the DOM), while requiring only minor quantitative variation of the model parameters.

## MATERIALS AND METHODS

### Isolation of mouse pancreatic islets

Experiments were carried out with male Swiss-Webster mice (25–30 g) from Charles River Laboratories (Wilmington, MA) or SUR1<sup>-/-</sup> mice (C57Bl/6 background) and littermate controls (SUR1<sup>+/+</sup>), which were generated by breeding heterozygous animals generously provided by Dr. David Piston (39). Mice were sacrificed by cervical dislocation according to the regulations of the University of Michigan Committee on Use and Care of Animals (UCUCA). Islets were isolated from the pancreas as in Zhang et al. (40), and maintained in culture for 1–2 days in RPMI1640 supplemented with 10% (v/v) fetal calf serum, 100 U/mL penicillin, and 100  $\mu\text{g}/\text{mL}$  streptomycin (Invitrogen, Carlsbad, CA).

### Electrophysiology

An Axopatch-200B patch-clamp amplifier (Axon Instruments, Union City, CA) was used in the perforated patch-clamp configuration to record membrane potential ( $V_m$ ). Islets were perfused with a standard external solution containing (in mM): 115 NaCl, 5 KCl, 3  $\text{CaCl}_2$ , 2  $\text{MgCl}_2$ , 10 HEPES, 11.1 glucose; pH 7.4. Pipette tips were filled with an internal solution (in mM): 28.4  $\text{K}_2\text{SO}_4$ , 63.7 KCl, 11.8 NaCl, 1  $\text{MgCl}_2$ , 20.8 HEPES, 0.5 EGTA; pH 7.2) containing 0.1 mg/mL amphotericin B.

### Monitoring metabolism using NAD(P)H fluorescence

To monitor changes in endogenous NAD(P)H levels (41–43), islets were placed in a glass-bottomed chamber (54  $\mu\text{L}$  volume) (Warner Instruments, Hamden, CT) on an Olympus IX-71 inverted microscope equipped with a 0.3 N.A. UPlanFL/UIS2 10 $\times$  objective (Olympus America, Center Valley, PA). The chamber was perfused at 0.3 mL/min and temperature was maintained at 33°C using inline and chamber heaters (Warner Instruments). The recording solution was either standard physiologic saline solution (in mM: 137 NaCl, 5 KCl, 1.2  $\text{MgCl}_2$ , 0.5  $\text{NaH}_2\text{PO}_4$ , 4.2  $\text{NaHCO}_3$ , 2.6  $\text{CaCl}_2$ , 10 HEPES, 2.8 glucose; pH 7.4, 310 mOsm), or higher (KCl) solutions using equimolar replacement of NaCl. Islet autofluorescence was elicited with

365 nm light (10 ms) using a Till Polychrome V monochromator (Till Photonics GmbH, Graefelfing, Germany), a UG11 (330/140) exciter, a 410DCLP beamsplitter, and a D500/100 wideband emission filter (Chroma Technology, Rockingham, VT). NAD(P)H emission was collected with a Photometrics QuantEM:512SC camera (Tucson, AZ) at 0.2 Hz. MetaFluor software (Molecular Devices, Downingtown, PA) was used for hardware control and online analysis. In experiments on SUR1<sup>-/-</sup> islets NAD(P)H was measured using a photomultiplier mounted on an Olympus IX-50 microscope under the control of IonWizard software (IonOptix, Milton, MA).

### Fura-2 imaging of intracellular calcium ( $[\text{Ca}^{2+}]_i$ )

Islets were loaded with 5  $\mu\text{M}$  Fura-2/AM (Invitrogen, Carlsbad, CA) for 20–30 min in a 95:5% air/ $\text{CO}_2$  incubator at 37°C, and then transferred to the recording chamber. The microscope configuration was similar to that used for NAD(P)H measurements, except that Fura-2 fluorescence was elicited by alternating excitation wavelengths of 340 and 380 nm. Changes in  $[\text{Ca}^{2+}]_i$  were expressed as 340:380 ratio, and offline analysis was carried out using MetaFluor software.

### Analysis of slow metabolic oscillations by fast Fourier transform

To determine the average period of slow NAD(P)H oscillations, islet fluorescence was measured using MetaFluor software. Data were linearly detrended to correct for photobleaching using IgorPro (Wavemetrics, Portland, Oregon), and the fast Fourier transform (FFT) function in the MATLAB Signal Processing Tool (The Mathworks, Natick, MA) was used to estimate power spectral density. Islets were categorized as oscillatory only if FFT detected a dominant period in recordings lasting >20 min, and nonoscillatory if periods of <1 min or >15 min were predominant. Islets classified as nonoscillatory by this criterion were also nonoscillatory by visual inspection. The dominant oscillatory period is reported for each islet.

### The DOM

The DOM is a mathematical model that has been developed to account for the diverse oscillatory patterns observed in islet membrane potential and  $\text{Ca}^{2+}$ . The model has been previously described in detail (34), so the description here is brief. The DOM consists of three interacting components representing glycolysis, mitochondrial metabolism, and plasma membrane electrical activity and intracellular  $\text{Ca}^{2+}$  handling. The glycolytic component can oscillate because of positive feedback onto phosphofructokinase-1 (PFK-1) by its product, fructose 1,6-bisphosphate (FBP). This increases enzyme activity until the substrate is decreased below the level that supports PFK-1 activity, reducing enzyme activity until substrate levels recover, initiating the next oscillation (44). These intrinsic glycolytic oscillations produce slow (~5 min) oscillations in mitochondrial ATP production, which in turn drive electrical oscillations through the  $\text{K}_{\text{ATP}}$  channels.

In addition to positive feedback onto PFK-1 by FBP, there is also negative feedback by ATP. In fact, the model predicts that oscillations are terminated if cytosolic [ATP] rises sufficiently. Thus, cytosolic ATP is an important modulator of PFK-1 in the DOM. Cytosolic ATP is determined by mitochondrial ATP production and ATP hydrolysis by various cellular processes. Some of these processes are  $\text{Ca}^{2+}$  dependent, such as the ATPases that move  $\text{Ca}^{2+}$  into the endoplasmic reticulum or out of the cell.

A key feature of the model is that the production of metabolic oscillations does not require  $\text{Ca}^{2+}$  oscillations; the oscillations are intrinsic to metabolism and can persist when  $\text{Ca}^{2+}$  is fixed. This is in contrast to models where  $\text{Ca}^{2+}$  oscillations are essential for metabolic oscillations, in which case cell hyperpolarization will always terminate the metabolic oscillations. The main goal of this study was to experimentally assess the effect of blockade of  $\text{Ca}^{2+}$  entry on the metabolic oscillations and compare the results obtained to predictions of the DOM.

Equations and values for all parameters except those listed in the legend for Fig. 1 are given in Bertram et al. (34). Computer code for the model can be downloaded from <http://www.math.fsu.edu/~bertram/software/islet>.

## RESULTS

### Mathematical models of islet oscillatory activity can be parsed by experiments using diazoxide to eliminate $\text{Ca}^{2+}$ oscillations

Fig. 1 shows the predictions of several mathematical models representing the effects of Dz on islet NAD(P)H oscillations in 11.1 mM glucose. The application of Dz is simulated in these models by maximizing  $G_{\text{K(ATP)}}$ , which is equivalent to opening all  $\beta$ -cell  $\text{K}_{\text{ATP}}$  channels. Fig. 1 A shows the prediction of a model equivalent to the simplest form of the Keizer-Magnus model (13). Inhibiting  $\text{Ca}^{2+}$  oscillations using this model abolishes metabolic oscillations because metabolic oscillations depend exclusively on pulsatile fluxes of  $\text{Ca}^{2+}$  across the mitochondrial inner membrane that in turn depolarize the mitochondrial membrane potential and inhibit ATP production. In the simulations shown for the

Keizer-Magnus model, metabolic oscillations appear as oscillations in ADP.

Fig. 1 B shows a similar result, in this case predicted by the model of Fridlyand et al. (32,33). In contrast to the Keizer-Magnus model,  $\text{Ca}^{2+}$  oscillations do not require metabolic oscillations (not shown), but in common with Keizer-Magnus, the metabolic oscillations result from periodic increases in cytosolic  $\text{Ca}^{2+}$ . In the Fridlyand model, pulsatile increases in cytosolic  $\text{Ca}^{2+}$  influence metabolism by increasing ATP consumption by  $\text{Ca}^{2+}$ - and  $\text{Na}^+/\text{K}^+$ -ATPases. Blocking  $\text{Ca}^{2+}$  influx using Dz thus abolishes NAD(P)H oscillations in this model, as for the Keizer-Magnus model. Thus, although the nature of the coupling is very different in these two models, the predicted responses to Dz are the same.

We next examined the DOM (see Materials and Methods) (34). In addition to a glycolytic oscillator, the DOM has an electrical oscillator driven by the feedback of cytosolic  $\text{Ca}^{2+}$  onto  $\text{Ca}^{2+}$ -activated  $\text{K}^+$  channels (45,46). This electrical oscillator, which is similar to that used to produce the  $[\text{Ca}^{2+}]_i$  oscillations depicted in Fig. 1, A and B, and equivalent to the simplest form of the Keizer-Magnus model (13),

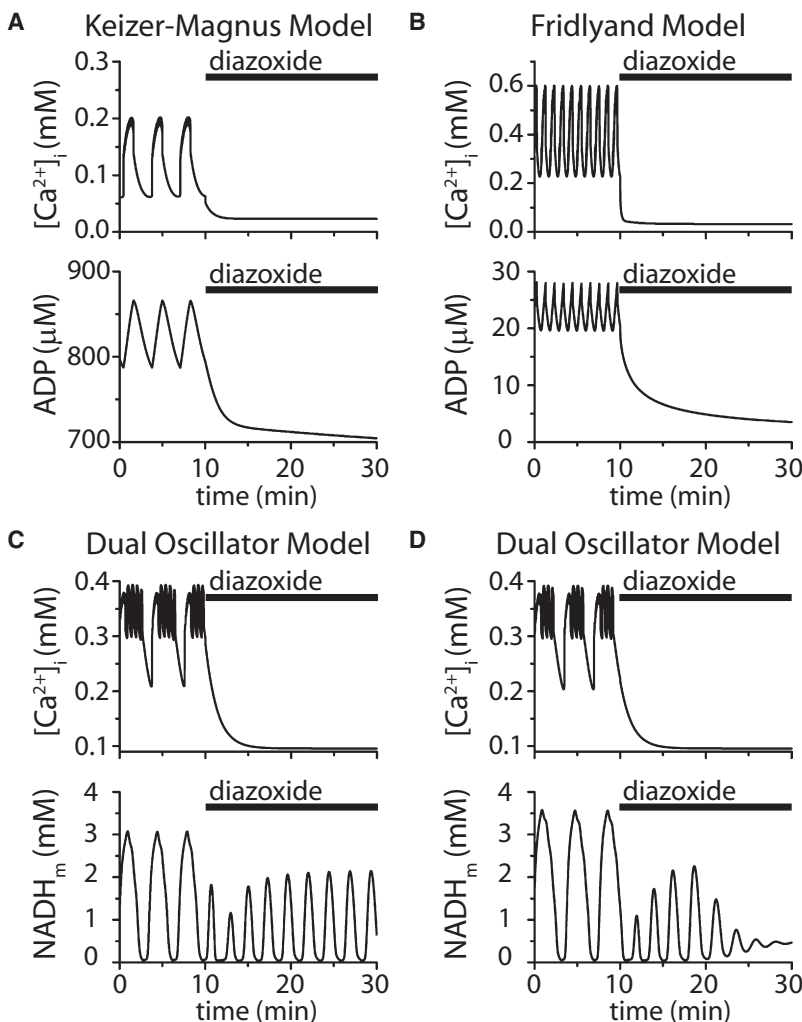


FIGURE 1 Simulated effects of the  $\text{K}_{\text{ATP}}$  channel-opener Dz on  $[\text{Ca}^{2+}]_i$  and metabolic oscillations with several mathematical models.  $[\text{Ca}^{2+}]_i$  is the free cytosolic  $\text{Ca}^{2+}$  concentration, and  $\text{NADH}_m$  is the mitochondrial NADH concentration. (A)  $[\text{Ca}^{2+}]_i$  and ADP for a model equivalent to the Keizer-Magnus model (13). ADP oscillations are abolished by Dz. (B)  $[\text{Ca}^{2+}]_i$  and ADP for the model of Fridlyand et al. (32). ADP oscillations are abolished by Dz. (C and D) Results with the DOM. The glucokinase reaction rate parameter  $J_{\text{GK}}$  in C is smaller than in D, but otherwise the models are identical. The metabolic oscillations in C persist with smaller amplitude when Dz is applied (all  $\text{K}_{\text{ATP}}$  channels put into an open state), whereas in D the metabolic oscillations are terminated. Parameter values that differ from those in Bertram et al. (34) are  $J_{\text{GK}} = 470 \mu\text{M ms}^{-1}$ ,  $k_4 = 330 \mu\text{M}$ ,  $g_{\text{K(Ca)}} = 250 \text{ pS}$ ,  $g_{\text{K(Ca)}} = 11,000 \text{ pS}$ , and  $g_k = 2000 \text{ pS}$ . Parameter values in D are the same as in C, except  $J_{\text{GK}} = 530 \mu\text{M ms}^{-1}$ .

produces fast bursts of electrical activity (period  $<1$  min) that are clustered into slower episodes by the glycolytic oscillator, producing compound bursting in  $[Ca^{2+}]_i$  (40,47–49). The model can also produce pure slow oscillations having the same response to Dz (not shown). Fig. 1, C and D, show compound  $Ca^{2+}$  oscillations produced using this model for two different values of the glucokinase reaction rate,  $J_{GK}$ . The slow component of the oscillations reflects glycolytic oscillations, which feed into mitochondrial metabolism to produce oscillations in NADH ( $NADH_m$ ) and ultimately, ATP. Dz again immediately hyperpolarizes the model islet, and cytosolic  $Ca^{2+}$  approaches a low basal level. The response of the metabolic oscillations to the cessation of  $Ca^{2+}$  oscillations, however, is different for the two islets simulated with the DOM. In one case (Fig. 1 C),  $NADH_m$  oscillations continue despite the continued presence of Dz, although they are reduced in amplitude. The metabolic oscillations persist because they are intrinsic, and reflect oscillatory glycolysis, which is not directly  $Ca^{2+}$  dependent. In the other case (Fig. 1 D), the  $NADH_m$  oscillations eventually dampen out when  $Ca^{2+}$  flux into the cell is abolished, so a loss of the  $Ca^{2+}$  oscillations in this case results in the cessation of metabolic oscillations. Here the metabolic oscillations are based on the same mechanism as in the simulation shown in Fig. 1 C, but they cease because Dz lowers mean cytosolic  $Ca^{2+}$ , which in turn reduces ATP use by the  $Ca^{2+}$  pumps, raising the ATP/ADP ratio (29) and inhibiting PFK-1 (50).

Whether blocking  $Ca^{2+}$  entry inhibits PFK-1-mediated metabolic oscillations or not in the DOM depends on the balance between PFK-1 inhibition by ATP and PFK-1 activation by its substrate. The two model islets shown in the figure differ in only one parameter value, the glucokinase reaction rate ( $J_{GK}$ ), which is larger in Fig. 1 D, leading to a larger mean ATP level, which in turn is able to suppress PFK-1-mediated oscillatory activity. The value of  $J_{GK}$  would depend on the glucose concentration and the level of glucokinase activity. Changes in other parameters (not shown), such as ones that affect the sensitivity of PFK-1 to ATP, can also convert a model islet with persistent metabolic oscillations (Fig. 1 C) into one in which oscillations die out after blocking  $Ca^{2+}$  entry (Fig. 1 D). We reiterate that in all other models published to date, with the exception of MacDonald et al. (28), the occurrence of  $Ca^{2+}$  oscillations is absolutely essential for metabolic oscillations to occur (25,26,29–32). Thus, finding intrinsic metabolic oscillations that persist when  $Ca^{2+}$  oscillations are abolished is an important prediction of the DOM (34,37).

The modeling shown in Fig. 2 shows further that the persistence of  $NADH_m$  oscillations is determined by the effects of ATP on PFK-1, which in turn depends on the level of  $Ca^{2+}$  and hence ATP use. Whereas this figure begins similarly to Fig. 1 D in that Dz abolishes  $NADH_m$  oscillations, in this case, KCl was increased after 60 min, raising the  $K^+$  equilibrium potential from  $-75$  mV to  $-50$  mV. This raises cytosolic  $Ca^{2+}$  (Fig. 2 A) and in turn lowers ATP (Fig. 2 B).

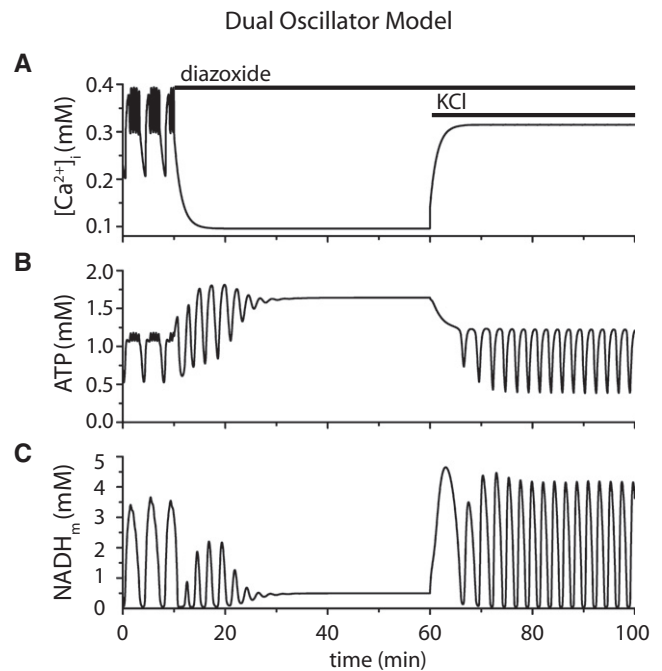


FIGURE 2 Predicted restoration of  $NADH_m$  oscillations. Continuation of simulation in Fig. 1 D with KCl added at  $t = 60$  min, simulated by raising the  $K^+$  reversal potential from  $-75$  mV to  $-50$  mV. The rise in  $[Ca^{2+}]_i$  (A) decreases free cytosolic ATP (B) and disinhibits PFK-1, which restores oscillations in  $NADH_m$  (C).

The consequent disinhibition of PFK-1 as ATP falls allows  $NADH_m$  oscillations to resume (Fig. 2 C). If KCl were raised further, ATP levels would be depressed further, and PFK-1 would be activated so strongly that it would stay on and no oscillations would be produced (not shown). Thus, the DOM predicts that increasing  $[Ca^{2+}]_i$  within a range of values should restore  $NADH_m$  oscillations in islets where they had been terminated initially by diazoxide application.

### Metabolic oscillations can persist without $[Ca^{2+}]_i$ oscillations

To test these predictions, slow oscillations in islet fuel metabolism were monitored by recording endogenous islet autofluorescence to 365 nm light, which reflects production of the reduced coenzymes NADH and NADPH, collectively referred to as NAD(P)H (18,41,51). Fig. 3 A shows representative slow NAD(P)H oscillations in six islets in 11.1 mM glucose. Simultaneous recording indicates the islets oscillated asynchronously. FFT was applied to each NAD(P)H time series to determine the underlying period. In 11.1 mM glucose, the dominant period of islet NAD(P)H oscillations was, on average,  $5.9 \pm 0.1$  min, with a median of 5.3 min ( $n = 133$  islets). This value is in good agreement with the previously reported period of  $5.1 \pm 0.1$  min (18). The oscillations were metabolic in origin as they were reversibly blocked by the glucokinase inhibitor D-mannoheptulose (5 mM) (Fig. S1 in the Supporting Material).

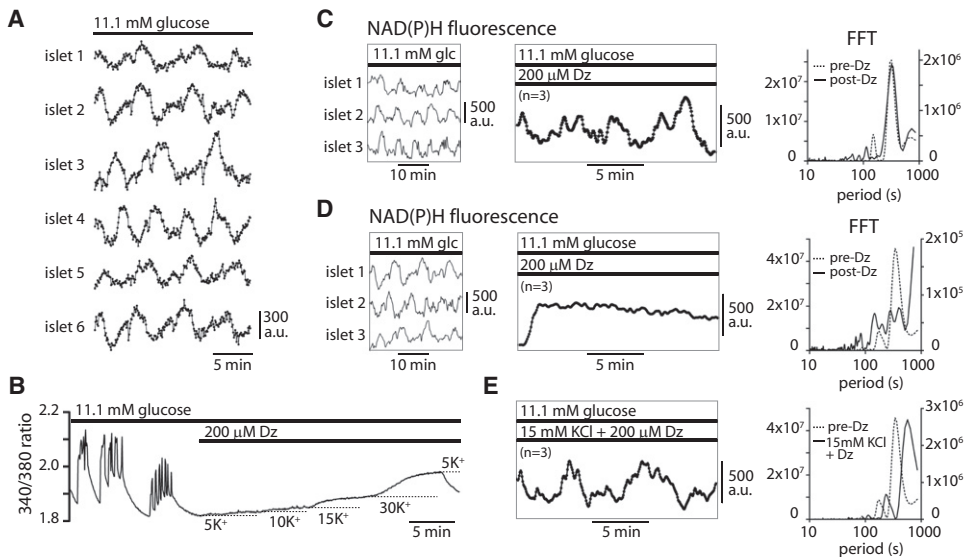


FIGURE 3 Islet NAD(P)H oscillations can occur without  $[Ca^{2+}]_i$  oscillations. (A) Oscillatory NAD(P)H fluorescence measured simultaneously from six islets in 11.1 mM glucose. Baseline-subtracted data are linearly detrended to correct for photobleaching. Representative traces are chosen from 133 islets measured in 26 independent experiments. (B) Blockage of islet  $[Ca^{2+}]_i$  oscillations with 200  $\mu$ M Dz as measured with Fura-2. Bath application of KCl was used to generate stepwise increases in  $[Ca^{2+}]_i$  ( $5K^+$ ,  $[K^+]_o = 5$  mM;  $10K^+$ ,  $[K^+]_o = 10$  mM; etc.). (C and D) Representative experiments showing the two outcomes observed for slow oscillations in NAD(P)H auto-fluorescence after Dz application. The left panels show NAD(P)H oscillations in 11.1 mM glucose before Dz application. In Dz (middle panels) NAD(P)H oscillations were either suppressed (representative of 67 islets) or persistent (representative of 34 islets). (E) For islets in which metabolic oscillations were initially suppressed by Dz (D, middle), subsequent elevation of  $[K^+]_o$  from 5 to 15 mM restored oscillations in 26 of 47 islets (54%) (E, left). The islets become synchronized in the presence of Dz; baseline-subtracted NAD(P)H traces averaging three islets in the same recording chamber are shown. (C–E) FFT spectra are displayed for NAD(P)H measurements taken either before (dashed lines, left axes) or after (solid lines, right axes) Dz application; the FFT of islet 3 is displayed as representative in each case.

As shown in Fig. 3 B, the application of 200  $\mu$ M Dz promptly abolished islet  $[Ca^{2+}]_i$  oscillations. Under these conditions, stepwise increases in extracellular  $K^+$  from 5 to 10, 15, and 30 mM, elevated mean  $[Ca^{2+}]_i$ , as expected, but did not restore  $[Ca^{2+}]_i$  oscillations. In parallel experiments monitoring NAD(P)H, 200  $\mu$ M Dz was applied to islets exhibiting slow metabolic oscillations in 11.1 mM glucose (Fig. 3, C and D). Two distinct types of islet responses to Dz were observed, as confirmed by FFT: 1), loss of NAD(P)H oscillations; and 2), persistent NAD(P)H oscillations having reduced amplitude.

Of 101 islets, 34 (34%) exhibited NAD(P)H oscillations that persisted in 200  $\mu$ M Dz, as in Fig. 3 C, although their amplitude was typically reduced to  $\sim$ 25% of controls. Interestingly, although NAD(P)H oscillations in separate islets were initially asynchronous, oscillations were synchronized by Dz ( $n = 203$  islets, measured in 33 independent experiments). Dz-induced synchronization of the islet metabolic oscillations is consistent with our observation that Dz similarly synchronized the  $Ca^{2+}$  oscillations of independent islets (52) (see also Fig. 5). Because of synchronization, we were able to increase the signal/noise ratio by analyzing averaged NAD(P)H fluorescence when Dz was present. In Fig. 3 C, middle, the averaged NAD(P)H oscillations from three islets measured in a single experiment are shown on an expanded scale to demonstrate their resemblance to the corresponding oscillations measured before Dz application (Fig. 3 C, left). FFT (exemplified by islet 3 in Fig. 3 C, right) indicated the period of these slow oscillations was not changed by Dz (pre-Dz,  $6.1 \pm 0.3$  min; post-Dz,  $5.6 \pm$

$0.3$  min;  $n = 34$ ,  $p = 0.29$  in a paired, two-tailed  $t$ -test). These data thus show that metabolic oscillations can occur in the complete absence of  $[Ca^{2+}]_i$  oscillations, indicating that they have an independent origin in at least a subset of islets. The DOM reproduces this behavior, including the reduction in the amplitude of NAD(P)H oscillations seen experimentally in the presence of Dz (Fig. 1 C).

For the remaining islets (67 of 101), Dz addition eliminated NAD(P)H oscillations (as in Fig. 3 D), as confirmed by FFT. The elimination of metabolic oscillations by Dz is consistent with previous reports (15,18).

One possible explanation for our finding that in some islet oscillations were eliminated whereas in others they persisted is simply that in some but not all islets  $Ca^{2+}$  oscillations are required for metabolic oscillations. However, as discussed earlier, in the DOM, metabolic oscillations are intrinsic to islets. They are eliminated by Dz because glycolytic PFK-1 is allosterically inhibited by the ATP that builds up as  $Ca^{2+}$ -ATPases switch off when the  $[Ca^{2+}]_i$  level falls sufficiently. The model then predicts that even if an islet is in a nonoscillatory state, a subsequent rise in  $Ca^{2+}$  could restore  $Ca^{2+}$ -ATPase activity by triggering increased consumption of ATP, disinhibiting PFK-1, and in turn restoring the metabolic oscillations (Fig. 2). When we tested this prediction by elevating extracellular KCl from 5 to 15 mM, which raised  $[Ca^{2+}]_i$  as shown in Fig. 3 B, NAD(P)H oscillations again became evident and persisted for  $>20$  min despite the continued presence of Dz (see Fig. 3 E, a continuation of the recording in Fig. 3 D). Oscillations were restored in 54% of islets (26 of 47) in which KCl was elevated in the

presence of Dz. This finding thus confirms what we believe to be a novel and, to date, unique prediction of the DOM.

Given the evidence for an intrinsic metabolic oscillator in islets, we reasoned that nonpharmacologic manipulations that decouple ionic from metabolic oscillations should produce similar results to those using Dz. Genetic loss of sulfonylurea receptor 1 (SUR1), a subunit of the  $K_{ATP}$  channel, results in  $\beta$ -cells in which electrical activity becomes uncoupled from fuel metabolism, and by extension, metabolic oscillations. To show this decoupling, we measured membrane potential ( $V_m$ ) and  $[Ca^{2+}]_i$  in islets from SUR1<sup>-/-</sup> and SUR1<sup>+/+</sup> littermate controls. As shown in Fig. 4 A, slow bursting in  $V_m$  was observed in SUR1<sup>+/+</sup> islets (period =  $3.7 \pm 0.4$  min,  $n = 8$ ) bathed in 11.1 mM glucose, whereas only continuous fast  $V_m$  spiking was observed in SUR1<sup>-/-</sup> islets that were cultured overnight in media containing 11.1 mM glucose ( $n = 8$ ). SUR1<sup>-/-</sup> islets ( $n = 8$ ) also lacked  $[Ca^{2+}]_i$  oscillations in 11.1 mM glucose under these conditions (Fig. 4 B). Culturing the islets overnight was critical to the experiment because we observed oscillations in electrical activity and  $[Ca^{2+}]_i$  in SUR1<sup>-/-</sup> islets cultured for  $\leq 4$  h (Fig. S2); this finding has been reported previously (53,54). In contrast, wild-type islets exhibited  $[Ca^{2+}]_i$  oscillations having a period of  $3.9 \pm 0.1$  min ( $n = 13$ ); this was not changed by overnight culturing. Most importantly, Fig. 4 C illustrates that slow oscillations in NAD(P)H in the SUR1<sup>+/+</sup> islets ( $4.9 \pm 0.4$  min,  $n = 17$ ,  $p > 0.05$ ) were not significantly different from those observed in SUR1<sup>-/-</sup> islets (period =  $4.4 \pm 0.3$  min,  $n = 19$ ), despite the absence of  $[Ca^{2+}]_i$  oscillations in these islets.

Thus, the data show that islet metabolic oscillations can persist whether islet  $[Ca^{2+}]_i$  oscillations are abolished pharmacologically or via genetic loss of  $K_{ATP}$  channels, suggest-

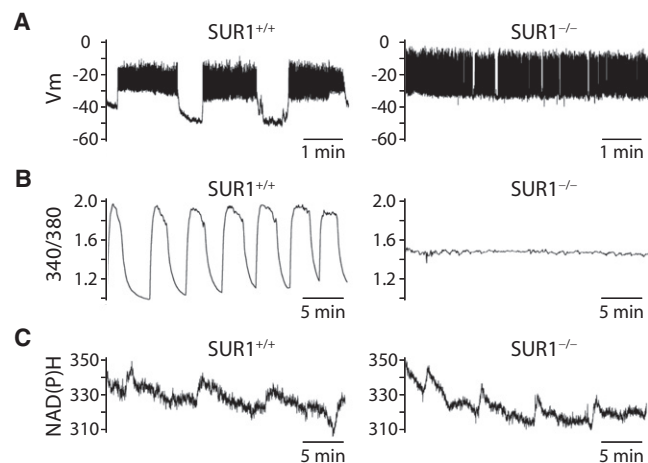


FIGURE 4 SUR1-null islets lacking functional  $K_{ATP}$  channels exhibit metabolic but not electrical oscillations. Representative recordings of (A) membrane potential ( $V_m$ ) ( $n = 8$ ), (B)  $[Ca^{2+}]_i$  (340:380 ratio) ( $n = 13$ ), and (C) NAD(P)H fluorescence ( $n = 19$  and  $17$ , respectively) are shown for SUR1<sup>-/-</sup> and SUR1<sup>+/+</sup> control islets, as indicated. All recordings were carried out in 11.1 mM glucose.

ing that the metabolic oscillator can function autonomously. We noted that these two sets of experiments differ in that the application of Dz results in low, nonoscillatory  $[Ca^{2+}]_i$ , whereas SUR1<sup>-/-</sup> islets exhibit high, nonoscillatory  $[Ca^{2+}]_i$  ( $243 \pm 20$  nM in 2.8 mM glucose) as compared to controls ( $72 \pm 11$  nM in 2.8 mM glucose,  $p < 0.0001$  in a two-tailed  $t$ -test,  $n = 8$ – $12$ ). Therefore, to more fully examine this point, we next tested the effects of elevated steady-state  $[Ca^{2+}]_i$  on slow NAD(P)H oscillations.

### Increases in nonoscillatory $[Ca^{2+}]_i$ and glucose modulate the slow metabolic oscillations

Whereas the data above show that  $[Ca^{2+}]_i$  oscillations are not mandatory for islet metabolic oscillations to occur, we observed that changing  $[Ca^{2+}]_i$  levels modulated the NAD(P)H oscillations of the islets (Fig. 5 A). Moderate elevations in nonoscillatory  $[Ca^{2+}]_i$  were achieved by increasing  $[K^+]_o$  from 5 to 15 mM (see Fig. 3 B) in the presence of Dz and 11.1 mM glucose.  $[Ca^{2+}]_i$  elevation did not change the period ( $[K^+]_o = 5$  mM,  $5.6 \pm 0.3$  min;  $[K^+]_o = 15$  mM,  $5.0 \pm 0.4$  min;  $n = 14$ ;  $p = 0.054$ ) or amplitude ( $[K^+]_o = 5$  mM,  $264 \pm 26$  a.u.;  $[K^+]_o = 15$  mM,  $288 \pm 24$  a.u.;  $n = 13$ ;  $p = 0.82$ ) of the NAD(P)H oscillations. However, increasing  $[K^+]_o$  to 30 mM produced a large transient rise of NAD(P)H, followed by a fall and then the resumption of oscillations exhibiting a  $\sim 60\%$  increase in both frequency (period =  $3.2 \pm 0.1$  min;  $p = 0.010$  in a paired, two-tailed  $t$ -test;  $n = 13$ ) and amplitude ( $456 \pm 48$  a.u.;  $p = 0.008$ ;  $n = 13$ ). This indicates that although  $Ca^{2+}$  oscillations were not required for the production of metabolic oscillations, increasing the  $Ca^{2+}$  level strongly enhanced them.

Finally, islets were first bathed in 2.8 mM glucose with Dz, and then glucose was increased to 11.1 mM while keeping Dz present (Fig. 5 B). This design allowed the metabolic effects of glucose to be tested in the absence of  $K_{ATP}$ -channel closure, and hence the absence of  $[Ca^{2+}]_i$  oscillations. Under this condition, only weak aperiodic fluctuations in baseline NAD(P)H fluorescence were apparent in 2.8 mM glucose and 200  $\mu$ M Dz. We have observed NAD(P)H oscillations in 2.8 mM glucose (not shown), but because the magnitude is likely to be further reduced by Dz, NAD(P)H oscillations in 2.8 mM glucose and Dz may be below the detection limit. Nonetheless, stimulating metabolism with 11.1 mM glucose resulted in a sharp increase in NAD(P)H fluorescence ( $41 \pm 0.02\%$ ;  $n = 27$ ) with superimposed NAD(P)H oscillations. This result further supports the hypothesis that oscillatory NAD(P)H does not require oscillatory  $[Ca^{2+}]_i$ , and suggests that the metabolic oscillations that occur in the absence of  $[Ca^{2+}]_i$  oscillations still require elevated glucose, as expected.

## DISCUSSION

Insulin secretion depends jointly on two distinct but interrelated  $\beta$ -cell functions, cytosolic  $Ca^{2+}$  homeostasis and

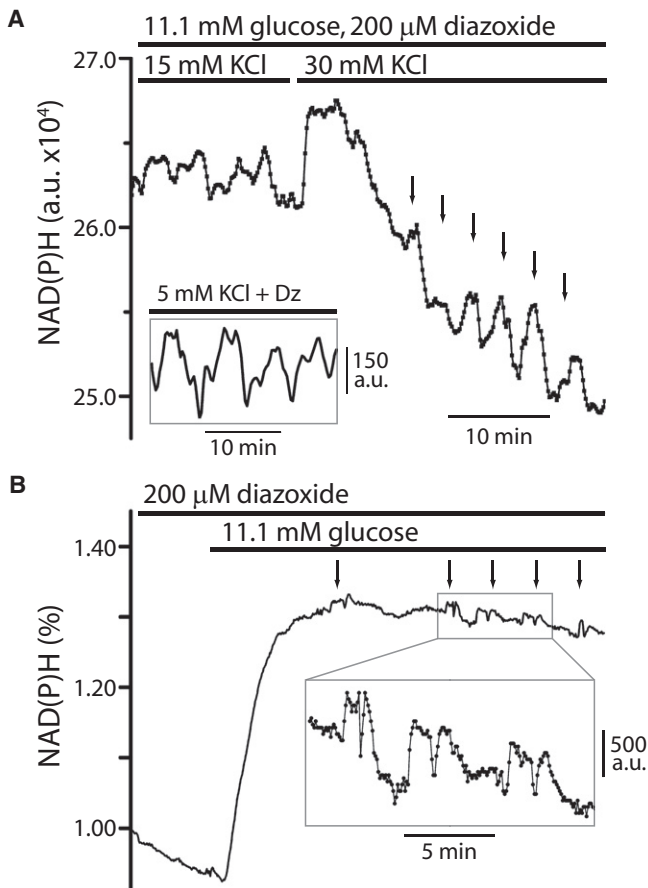


FIGURE 5 NAD(P)H oscillations are modulated by elevations of non-oscillatory  $[Ca^{2+}]_i$  or glucose. (A) Effect of elevating non-oscillatory  $[Ca^{2+}]_i$  on slow NAD(P)H oscillations measured in the continuous presence of 11.1 mM glucose and 200  $\mu$ M Dz.  $[Ca^{2+}]_i$  was elevated by increasing  $[K^+]_o$  in the bath as in Fig. 3 B. The representative trace is an average of four synchronized islets in the same chamber (in total, 13 islets were recorded in three independent experiments). The raw data traces are provided in Fig. S3 to illustrate islet synchronization. (B) Averaged change in islet NAD(P)H fluorescence from eight synchronized islets in the same recording chamber when glucose was elevated from 2.8 to 11.1 mM in the presence of 200  $\mu$ M Dz to clamp islet  $[Ca^{2+}]_i$ . Arrows indicate peaks of NAD(P)H oscillations. Scale bar is displayed for the inset graph. Trace is representative of 25 islets recorded in three independent experiments.

glucose metabolism. The  $Ca^{2+}$  component is largely shared with the universal exocytotic machinery that operates in hormone secretion from other endocrine cells and transmitter release from neurons. The metabolic component is specific to  $\beta$ -cells, which metabolize glucose and increase their ATP/ADP ratio in accord with the plasma glucose concentration, and not just their own metabolic requirements, befitting their role as metabolic sensors for the organism. Although the interrelationship between  $Ca^{2+}$  and metabolism is complex and unlikely to be completely dissociable, using the DOM as a tool for predicting islet oscillatory behavior, we sought experiments to rectify disagreement over which serves a pacemaker-like function.

Using endogenous NAD(P)H fluorescence, we analyzed the effects of abolishing islet  $[Ca^{2+}]_i$  oscillations with Dz on islet metabolic oscillations. In many of the islets (34%) the metabolic oscillations persisted in the complete absence of  $Ca^{2+}$  oscillations. In the remainder (66%), Dz eliminated the metabolic oscillations, but increases in steady-state  $[Ca^{2+}]_i$  produced by raising  $[K^+]_o$  could, in most cases (26 of 47 tested; 54%), restore the metabolic oscillations. Although  $Ca^{2+}$  and NAD(P)H were not measured simultaneously, the  $[Ca^{2+}]_i$  oscillations were invariably eliminated by Dz. Therefore,  $[Ca^{2+}]_i$  oscillations are not required to produce islet metabolic oscillations in islets. This is further supported by our demonstration that NAD(P)H oscillations persisted in SUR1-null mice, which lack the  $K_{ATP}$  channels that serve as the main metabolic sensor of the  $\beta$ -cell, and therefore lack  $Ca^{2+}$  and electrical oscillations under the experimental conditions we used.

Moreover, the finding that metabolic oscillations can occur in the absence of  $Ca^{2+}$  oscillations is consistent with models in which the  $\beta$ -cell metabolic oscillator is glycolytic in origin (34–37). In contrast, the data are inconsistent with the class of islet models in which metabolic oscillations are driven exclusively by  $Ca^{2+}$  feedback (25,26,29–32), because in these models terminating the  $Ca^{2+}$  oscillations necessarily terminates the metabolic oscillations. Whereas we showed previously (34) that the observation that Dz abolishes oscillations in metabolic variables such as oxygen consumption or NAD(P)H does not rule out oscillations intrinsic to metabolism, this study shows that models in which metabolic oscillations are secondary to  $[Ca^{2+}]_i$  oscillations are incorrect, or at best incomplete. However, those models may still be viable candidates for the electrical subcomponent of the DOM. Indeed, our model contains a form of the Keizer-Magnus model as a submodel. In Keizer-Magnus, the influx of  $Ca^{2+}$  reduces ATP/ADP, leading in turn to the opening of  $K_{ATP}$  channels. In our view, this is part of the ionic or electrical component, which can coexist with the slow, intrinsic metabolic oscillatory mechanism.

Although we have shown that  $[Ca^{2+}]_i$  oscillations are not necessary for the production of metabolic oscillations,  $Ca^{2+}$  was found to be an important modulator of the oscillations. For example, in those islets in which metabolic oscillations persisted in the presence of Dz, their amplitude was reduced, consistent with the predictions of the DOM. When the islets were subsequently depolarized with 30 mM  $[K^+]_o$ , leading to an increase in mean  $[Ca^{2+}]_i$ , the amplitude of the NAD(P)H oscillations correspondingly increased. Clearly, then, the  $[Ca^{2+}]_i$  level has a significant influence on islet metabolic oscillations, even if it is not the driver of those oscillations. These observations confirm an additional specific prediction of the DOM, and are in good agreement with a large body of literature indicating that  $[Ca^{2+}]_i$  can strongly amplify metabolism. In other studies, oscillations in  $O_2$  consumption were similarly reduced in amplitude by the removal of external  $Ca^{2+}$  (in HIT  $\beta$ -cells) (55) or by

blocking L-type  $\text{Ca}^{2+}$  channels with nifedipine (in mouse islets) (56). The observed effect of  $\text{Ca}^{2+}$  to enhance metabolic oscillations is not surprising, because  $\text{Ca}^{2+}$  activates mitochondrial dehydrogenases (27,28).  $\text{Ca}^{2+}$  flux across the mitochondrial inner membrane can also reduce mitochondrial membrane potential, diminishing ATP/NADH production (25,26). Equally important in our model is the direct relationship between ATP consumption via  $\text{Ca}^{2+}$ -ATPases (29,30) and the activity of PFK-1 and glycolytic flux (35). Through these mechanisms,  $[\text{Ca}^{2+}]_i$  need not oscillate but may need to be elevated for robust metabolism, which is illustrated by our demonstration that oscillations could be restored by a moderate elevation of  $\text{Ca}^{2+}$  in those islets in which the slow NAD(P)H oscillations were initially abolished by Dz. In addition, we make no claim to have proven that islet metabolic oscillations are glycolytic, as the slow oscillations in NAD(P)H we observed experimentally could in principle reflect either glycolytic or mitochondrial processes (42). However, the results are consistent with the DOM, in which metabolic oscillations generated by glycolysis are amplified via the mitochondria, and argue strongly against any model that excludes a role for intrinsic metabolic oscillations.

In summary, we have shown that the pacemaker that underlies slow islet oscillations is metabolic in origin rather than  $\text{Ca}^{2+}$ -driven. This does not mean that  $\text{Ca}^{2+}$  is unimportant, as it was found to enhance the metabolic oscillations, is the trigger for insulin granule exocytosis, and provides feedback onto  $\beta$ -cell  $\text{K}^+$  channels that are most likely responsible for the bursts of electrical activity that are clustered into episodes by the metabolic oscillator (34,37). As raising  $\text{Ca}^{2+}$  triggers exocytosis (e.g., using sulfonylureas or KCl) but is insufficient for full activation of sustained insulin secretion (57), an integrated view of the interrelationships of islet  $\text{Ca}^{2+}$  and metabolism will be essential for the development of balanced secretagogue therapy for the successful treatment of patients with diabetes.

## SUPPORTING MATERIAL

Three figures are available at [http://www.biophysj.org/biophysj/supplemental/S0006-3495\(10\)00473-X](http://www.biophysj.org/biophysj/supplemental/S0006-3495(10)00473-X).

We thank Mary Clark for preparation of mouse islets.

This work is supported by the National Institutes of Health (RO1-DK46409 to L.S.S.), the National Institute of Diabetes and Digestive and Kidney Diseases (F32-DK085960 to M.J.M.), the American Heart Association (AHA-0715126 to B.F.), and the National Science Foundation (DMS-0613179; DMS-0613179 and DMS-0917664 to R.B.).

## REFERENCES

- Pørksen, N. 2002. The in vivo regulation of pulsatile insulin secretion. *Diabetologia*. 45:3–20.
- Nunemaker, C. S., M. Zhang, ..., L. S. Satin. 2005. Individual mice can be distinguished by the period of their islet calcium oscillations: is there an intrinsic islet period that is imprinted in vivo? *Diabetes*. 54: 3517–3522.
- Lang, D. A., D. R. Matthews, ..., R. C. Turner. 1981. Brief, irregular oscillations of basal plasma insulin and glucose concentrations in diabetic man. *Diabetes*. 30:435–439.
- Song, S. H., S. S. McIntyre, ..., P. C. Butler. 2000. Direct measurement of pulsatile insulin secretion from the portal vein in human subjects. *J. Clin. Endocrinol. Metab.* 85:4491–4499.
- Matveyenko, A. V., J. D. Veldhuis, and P. C. Butler. 2008. Measurement of pulsatile insulin secretion in the rat: direct sampling from the hepatic portal vein. *Am. J. Physiol.* 295:E569–E574.
- Gilon, P., R. M. Shepherd, and J. C. Henquin. 1993. Oscillations of secretion driven by oscillations of cytoplasmic  $\text{Ca}^{2+}$  as evidences in single pancreatic islets. *J. Biol. Chem.* 268:22265–22268.
- Matthews, D. R., D. A. Lang, ..., R. C. Turner. 1983. Control of pulsatile insulin secretion in man. *Diabetologia*. 24:231–237.
- O’Rahilly, S., R. C. Turner, and D. R. Matthews. 1988. Impaired pulsatile secretion of insulin in relatives of patients with non-insulin-dependent diabetes. *N. Engl. J. Med.* 318:1225–1230.
- Polonsky, K. S., B. D. Given, ..., E. Van Cauter. 1988. Abnormal patterns of insulin secretion in non-insulin-dependent diabetes mellitus. *N. Engl. J. Med.* 318:1231–1239.
- Dean, P. M., and E. K. Matthews. 1970. Glucose-induced electrical activity in pancreatic islet cells. *J. Physiol.* 210:255–264.
- Ashcroft, F. M., D. E. Harrison, and S. J. H. Ashcroft. 1984. Glucose induces closure of single potassium channels in isolated rat pancreatic  $\beta$ -cells. *Nature*. 312:446–448.
- Cook, D. L., and C. N. Hales. 1984. Intracellular ATP directly blocks  $\text{K}^+$  channels in pancreatic B-cells. *Nature*. 311:271–273.
- Keizer, J., and G. Magnus. 1989. ATP-sensitive potassium channel and bursting in the pancreatic beta cell. A theoretical study. *Biophys. J.* 56:229–242.
- Longo, E. A., K. Tornheim, ..., B. E. Corkey. 1991. Oscillations in cytosolic free  $\text{Ca}^{2+}$ , oxygen consumption, and insulin secretion in glucose-stimulated rat pancreatic islets. *J. Biol. Chem.* 266:9314–9319.
- Kennedy, R. T., L. M. Kauri, ..., S. K. Jung. 2002. Metabolic oscillations in  $\beta$ -cells. *Diabetes*. 51 (Suppl 1):S152–S161.
- Ortsäter, H., P. Liss, ..., P. Bergsten. 2000. Oscillations in oxygen tension and insulin release of individual pancreatic *ob/ob* mouse islets. *Diabetologia*. 43:1313–1318.
- Bergsten, P., J. Westerlund, ..., P. O. Carlsson. 2002. Primary in vivo oscillations of metabolism in the pancreas. *Diabetes*. 51:699–703.
- Luciani, D. S., S. Misler, and K. S. Polonsky. 2006.  $\text{Ca}^{2+}$  controls slow NAD(P)H oscillations in glucose-stimulated mouse pancreatic islets. *J. Physiol.* 572:379–392.
- Nunemaker, C. S., and L. S. Satin. 2004. Comparison of metabolic oscillations from mouse pancreatic beta cells and islets. *Endocrine*. 25:61–67.
- Kindmark, H., M. Köhler, ..., P. O. Berggren. 2001. Glucose-induced oscillations in cytoplasmic free  $\text{Ca}^{2+}$  concentration precede oscillations in mitochondrial membrane potential in the pancreatic  $\beta$ -cell. *J. Biol. Chem.* 276:34530–34536.
- Juntti-Berggren, L., D.-L. Webb, ..., P. O. Berggren. 2003. Dihydroxyacetone-induced oscillations in cytoplasmic free  $\text{Ca}^{2+}$  and the ATP/ADP ratio in pancreatic  $\beta$ -cells at substimulatory glucose. *J. Biol. Chem.* 278:40710–40716.
- Nilsson, T., V. Schultz, ..., K. Tornheim. 1996. Temporal patterns of changes in ATP/ADP ratio, glucose 6-phosphate and cytoplasmic free  $\text{Ca}^{2+}$  in glucose-stimulated pancreatic  $\beta$ -cells. *Biochem. J.* 314:91–94.
- Ainscow, E. K., and G. A. Rutter. 2002. Glucose-stimulated oscillations in free cytosolic ATP concentration imaged in single islet  $\beta$ -cells: evidence for a  $\text{Ca}^{2+}$ -dependent mechanism. *Diabetes*. 51 (Suppl 1): S162–S170.

24. Chou, H.-F., N. Berman, and E. Ipp. 1992. Oscillations of lactate released from islets of Langerhans: evidence for oscillatory glycolysis in  $\beta$ -cells. *Am. J. Physiol.* 262:E800–E805.
25. Magnus, G., and J. Keizer. 1997. Minimal model of  $\beta$ -cell mitochondrial  $\text{Ca}^{2+}$  handling. *Am. J. Physiol.* 273:C717–C733.
26. Magnus, G., and J. Keizer. 1998. Model of  $\beta$ -cell mitochondrial calcium handling and electrical activity. I. Cytoplasmic variables. *Am. J. Physiol.* 274:C1158–C1173.
27. Civelek, V. N., J. T. Deeney, ..., B. E. Corkey. 1996. Regulation of pancreatic beta-cell mitochondrial metabolism: influence of  $\text{Ca}^{2+}$ , substrate and ADP. *Biochem. J.* 318:615–621.
28. MacDonald, M. J., L. A. Fahien, ..., M. A. Kendrick. 2003. Citrate oscillates in liver and pancreatic beta cell mitochondria and in INS-1 insulinoma cells. *J. Biol. Chem.* 278:51894–51900.
29. Detimary, P., P. Gilon, and J. C. Henquin. 1998. Interplay between cytoplasmic  $\text{Ca}^{2+}$  and the ATP/ADP ratio: a feedback control mechanism in mouse pancreatic islets. *Biochem. J.* 333:269–274.
30. Henquin, J. C. 1990. Glucose-induced electrical activity in beta-cells. Feedback control of ATP-sensitive  $\text{K}^+$  channels by  $\text{Ca}^{2+}$ ? [corrected]. *Diabetes.* 39:1457–1460.
31. Diederichs, F. 2006. Mathematical simulation of membrane processes and metabolic fluxes of the pancreatic  $\beta$ -cell. *Bull. Math. Biol.* 68:1779–1818.
32. Fridlyand, L. E., N. Tamarina, and L. H. Phillipson. 2003. Modeling the  $\text{Ca}^{2+}$  flux in pancreatic  $\beta$ -cells: role of the plasma membrane and intracellular stores. *Am. J. Physiol.* 285:E138–E154.
33. Fridlyand, L. E., L. Ma, and L. H. Phillipson. 2005. Adenine nucleotide regulation in pancreatic beta-cells: modeling of ATP/ADP- $\text{Ca}^{2+}$  interactions. *Am. J. Physiol. Endocrinol. Metab.* 289:E839–E848.
34. Bertram, R., L. S. Satin, ..., A. Sherman. 2007. Interaction of glycolysis and mitochondrial respiration in metabolic oscillations of pancreatic islets. *Biophys. J.* 92:1544–1555.
35. Tornheim, K. 1997. Are metabolic oscillations responsible for normal oscillatory insulin secretion? *Diabetes.* 46:1375–1380.
36. Tornheim, K. 1979. Oscillations of the glycolytic pathway and the purine nucleotide cycle. *J. Theor. Biol.* 79:491–541.
37. Bertram, R., A. Sherman, and L. S. Satin. 2007. Metabolic and electrical oscillations: partners in controlling pulsatile insulin secretion. *Am. J. Physiol.* 293:E890–E900.
38. Dryselius, S., P. E. Lund, ..., B. Hellman. 1994. Variations in ATP-sensitive  $\text{K}^+$  channel activity provide evidence for inherent metabolic oscillations in pancreatic beta-cells. *Biochem. Biophys. Res. Commun.* 205:880–885.
39. Shiota, C., O. Larsson, ..., M. A. Magnuson. 2002. Sulfonylurea receptor type 1 knock-out mice have intact feeding-stimulated insulin secretion despite marked impairment in their response to glucose. *J. Biol. Chem.* 277:37176–37183.
40. Zhang, M., P. Goforth, ..., L. Satin. 2003. The  $\text{Ca}^{2+}$  dynamics of isolated mouse  $\beta$ -cells and islets: implications for mathematical models. *Biophys. J.* 84:2852–2870.
41. Rocheleau, J. V., W. S. Head, and D. W. Piston. 2004. Quantitative NAD(P)H/flavoprotein autofluorescence imaging reveals metabolic mechanisms of pancreatic islet pyruvate response. *J. Biol. Chem.* 279:31780–31787.
42. Patterson, G. H., S. M. Knobel, ..., D. W. Piston. 2000. Separation of the glucose-stimulated cytoplasmic and mitochondrial NAD(P)H responses in pancreatic islet beta cells. *Proc. Natl. Acad. Sci. USA.* 97:5203–5207.
43. Piston, D. W., B. R. Masters, and W. W. Webb. 1995. Three-dimensionally resolved NAD(P)H cellular metabolic redox imaging of the in situ cornea with two-photon excitation laser scanning microscopy. *J. Microsc.* 178:20–27.
44. Smolen, P. 1995. A model for glycolytic oscillations based on skeletal muscle phosphofructokinase kinetics. *J. Theor. Biol.* 174:137–148.
45. Göpel, S. O., T. Kanno, ..., P. Rorsman. 1999. Activation of  $\text{Ca}^{2+}$ -dependent  $\text{K}^+$  channels contributes to rhythmic firing of action potentials in mouse pancreatic  $\beta$  cells. *J. Gen. Physiol.* 114:759–770.
46. Goforth, P. B., R. Bertram, ..., L. S. Satin. 2002. Calcium-activated  $\text{K}^+$  channels of mouse  $\beta$ -cells are controlled by both store and cytoplasmic  $\text{Ca}^{2+}$ : experimental and theoretical studies. *J. Gen. Physiol.* 130:307–322.
47. Beauvois, M. C., C. Merezak, ..., P. Gilon. 2006. Glucose-induced mixed  $[\text{Ca}^{2+}]_c$  oscillations in mouse  $\beta$ -cells are controlled by the membrane potential and the SERCA3  $\text{Ca}^{2+}$ -ATPase of the endoplasmic reticulum. *Am. J. Physiol.* 290:C1503–C1511.
48. Bergsten, P., E. Grapengiesser, ..., B. Hellman. 1994. Synchronous oscillations of cytoplasmic  $\text{Ca}^{2+}$  and insulin release in glucose-stimulated pancreatic islets. *J. Biol. Chem.* 269:8749–8753.
49. Valdeolmillos, M., R. M. Santos, ..., L. M. Rosario. 1989. Glucose-induced oscillations of intracellular  $\text{Ca}^{2+}$  concentration resembling bursting electrical activity in single mouse islets of Langerhans. *FEBS Lett.* 259:19–23.
50. Tornheim, K., and J. M. Lowenstein. 1974. The purine nucleotide cycle. IV. Interactions with oscillations of the glycolytic pathway in muscle extracts. *J. Biol. Chem.* 249:3241–3247.
51. Bennett, B. D., T. L. Jetton, ..., D. W. Piston. 1996. Quantitative subcellular imaging of glucose metabolism within intact pancreatic islets. *J. Biol. Chem.* 271:3647–3651.
52. Zhang, M., B. Fendler, ..., L. Satin. 2008. Long lasting synchronization of calcium oscillations by cholinergic stimulation in isolated pancreatic islets. *Biophys. J.* 95:4676–4688.
53. Düfer, M., D. Haspel, ..., G. Drews. 2004. Oscillations of membrane potential and cytosolic  $\text{Ca}^{2+}$  concentration in SUR1<sup>(-/-)</sup> beta cells. *Diabetologia.* 47:488–498.
54. Haspel, D., P. Krippeit-Drews, ..., M. Düfer. 2005. Crosstalk between membrane potential and cytosolic  $\text{Ca}^{2+}$  concentration in beta cells from Sur1<sup>-/-</sup> mice. *Diabetologia.* 48:913–921.
55. Porterfield, D. M., R. F. Corkey, ..., B. E. Corkey. 2000. Oxygen consumption oscillates in single clonal pancreatic  $\beta$ -cells (HIT). *Diabetes.* 49:1511–1516.
56. Jung, S.-K., C. A. Aspinwall, and R. T. Kennedy. 1999. Detection of multiple patterns of oscillatory oxygen consumption in single mouse islets of Langerhans. *Biochem. Biophys. Res. Commun.* 259:331–335.
57. Henquin, J. C. 2000. Triggering and amplifying pathways of regulation of insulin secretion by glucose. *Diabetes.* 49:1751–1760.